

Papers

Effects of Noise on Transients of Injection Locked Semiconductor Lasers

Marc R. Surette, Dag Roar Hjelme, *Member, IEEE*, Reinold Ellingsen,
and Alan Rolf Mickelson, *Member, IEEE*

Abstract—An analysis of transients of semiconductor laser injection locking is presented. The analysis is based on the semiconductor rate equations and includes the effects of noise, amplitude phase coupling, carrier dynamics, and gain saturation. By adiabatically eliminating the carrier dynamics, a single nonlinear stochastic differential equation is obtained for the relative phase between the master and slave lasers. The validity of the adiabatic approximation is verified by numerically integrating the rate equations. The corresponding Fokker-Planck equation is used to study the steady-state locked condition as well as phase transients of the locking process. Noise causes the steady-state relative phase between the master and the slave lasers to be a random variable with a standard deviation of approximately a few degrees for typical injection levels. The standard deviation can be reduced by using a phase detector with a limited bandwidth. The mean locking time in the presence of noise is slightly less than the deterministic prediction. Noise also causes the locked lasers to have a finite probability to momentarily unlock, equivalent to a particle escaping over a potential barrier. The results of an experimental measurement of the locking time is presented. As predicted by the analysis, the locking time is reduced by either increasing the locking bandwidth or reducing the free running frequency difference.

I. INTRODUCTION

IN high bandwidth applications utilizing injection locked semiconductor lasers, it is vital to understand the transient response of the locking process. Even if an application uses "steady-state" injection locking, the relative phase between the locked lasers is a random variable due to spontaneous emission noise. In this paper we investigate, analytically and experimentally, the transients of injection locked semiconductor lasers in the presence of noise.

The observation of injection locking of oscillators can be traced back to 1665 when Huygens observed his wall

Manuscript received December 23, 1991; revised November 9, 1992. This work was supported by the Office of Naval Research under Contract N00014-88-K-0685, the Army Research Office under Contract DAAL03-88-K-0053, and the Optoelectronic Computing Systems Center at the University of Colorado, Boulder. The work of R. Ellingsen was supported by the Norwegian Council for Scientific and Industrial Research. The numerical simulations were run on a Cray Y-MP under a Grant from the National Center for Supercomputing Applications.

M. R. Surette, D. R. Hjelme, and A. R. Mickelson are with the Department of Electrical and Computer Engineering, University of Colorado, Boulder, CO 80309.

R. Ellingsen is with SINTEF DELAB, Trondheim, Norway.
IEEE Log Number 9207470.

clocks for several days. The original analysis of injection locking was certainly not done by Huygens since Newton's *Principia Mathematica* was not published until 1687. Probably the earliest theoretical development of locking was present by Van der Pol in 1927 [1]. Van der Pol described the frequency locking of electrical oscillators. Nearly two decades later, Adler published a paper which provided a clear understanding of frequency locking phenomena [2]. The paper presented a nonlinear differential equation for the phase of an electrical oscillator relative to an injected signal. Adler showed that the locking bandwidth was inversely proportional to the square root of the injected power. Also, Adler discussed that the locked relative phase between the master and the slave depends on the injected power. The analysis in his paper described the transient of the relative phase as injection locking occurs. To date, the study of transients in injection locked oscillators has been limited to the deterministic solution of Adler's equation [2].

Apart from Adler, some other researchers investigated the phase and frequency transients in electrical oscillators. White and Jones provided a description of the frequency transients by differentiating Adler's closed form solution for the relative phase [3]. Earlier, Lisitsian [4] discussed frequency transients in oscillators by using numerical methods on a set of differential equations which described an oscillator. Takayama [5] investigated locking properties in injection locked nonlinear power amplifiers. He found the nonlinear admittance effects resulted in phase transients that varied slightly from Adler's theory. Also, experimental work has been published [6] and [7]. A good survey of the work done on electrical oscillators was published by Kurokawa [8]. In addition to electrical oscillators, the research of phase locked loops has provided much insight into the field of locking phenomena. The analytical results of phase locked loops are similar to the results obtained in other areas of locking research [9], [10].

It was not until 1966 that laser injection locking was demonstrated by Stover and Steiner [11]. Buczek *et al.* provided a review of the theory and applications of laser injection locking [12]. In the late 1970's, improvements in semiconductor laser characteristics such as improved

spectral purity and mode stability provided motivation for injection locking these lasers. The first demonstration of semiconductor laser injection locking was presented in a paper by Kobayashi and Kimura in 1980 [13].

The first applications of injection locking semiconductor lasers were for optical communications. It was shown that it was possible to modulate an injection locked semiconductor laser and maintain single-mode operation [14]–[17]. It has been suggested to use injection locking to synchronize local oscillators in coherent optical communication systems [18]. It has been shown that optical phase modulation can be obtained by modulating the injection locked slave [19]. Kikuchi *et al.* also utilized sideband injection locking in a wavelength division multiplexed coherent communication application.

Other research groups performed experiments to determine the effects of injection locking on modulation of semiconductor lasers. Goldberg *et al.* experimentally investigated the effect of injection locking on the modulation characteristics of laser array [20] as well as the control of spatial characteristics of the output of laser arrays [21]. Elze *et al.* [22] experimentally investigated the modulation properties of lasers stabilized by external cavities or injection locking.

In another related area, injection locked semiconductor lasers were used to generate stable microwave signals for various microwave applications [23], [24].

In parallel with the development of applications, the theory of semiconductor laser locking has evolved. The theoretical developments for semiconductor laser locking began in the early 1980's. Otsuka discussed injection locking in 1981 [25]. Lang pointed out that including the linewidth enhancement factor was necessary for the theoretical developments of injection locked semiconductor lasers [26].

Lang, and others, also discussed the stability of an injection locked semiconductor laser [27], [28]–[31]. The linear stability analysis of the semiconductor rate equations shows that for certain operating conditions within the locking bandwidth, the slave will be unstable. Different research groups have measured the resulting asymmetric stable locking bandwidth [32]–[34].

In a semiclassical analysis of a laser, that is treating the electric field classically and the gain medium quantum mechanically, the noise due to spontaneous emission, carrier generation and recombination is included in the rate equations by adding appropriate Langevin driving terms [35]. Some work on the effects of noise for injection locked semiconductor lasers has appeared in the literature [36]–[41]. In these papers, the effects of injection locking on the linewidth or the frequency spectral noise density of the slave laser was determined. Haus and Yamamoto also investigated noise properties of an injection locked laser oscillator [42]. Their analysis utilized the Fokker-Planck equation and the Langevin rate equation to describe phase fluctuations in the slave laser.

Most of the theoretical results were obtained assuming that the injected signal was weak. However, care must be

used when extending the analysis to strong injection. There has been some recent work on the effects of strong injection [43], [44]. Both these papers used a propagation based theory, whereas most of the earlier papers use a rate equation approach. However, as Tromborg *et al.* pointed out in the introduction of their paper [43] the rate equation approach adequately predicts experimental observations of injection locking properties for weak injection [27], [28].

None of the experimental or theoretical studies mentioned above have dealt with transients of the locking process. Besides the work of Spano *et al.* [45], we are not aware of any work on transients in injection locked semiconductor lasers. Spano *et al.* [45] have published a paper discussing the numerical results of integrating the rate equations to obtain phase transients in injection locked semiconductor lasers. For applications of optical frequency shift keying (FSK), they found that the main limitation was due to the time duration of the phase transient (10 ns for some anomalous cases). The rise time and fall time of the injected signal was set to zero, and in this limit they stated that the turn-off transient of the slave is equivalent to the damping of relaxation oscillations. It was the damping of the relaxation oscillations which limited the bandwidth of the FSK communication system.

In this paper we investigate the phase (frequency) transients of the slave as locking occurs. As discussed above, there has been some theoretical and experimental work on transients done in the past for electrical oscillators, where the transient response was described fairly well by Adler's theory, with some deviations. It is clear that one cannot assume beforehand that Adler's locking analysis will describe transients in semiconductor laser locking.

Our analysis is slightly different from these previously reported analyses since we are primarily concerned with injection locking transients. The difference between our noise analysis and the papers just mentioned is that a Langevin noise source is derived for the phase difference between the master and the slave. This allows us to write a stochastic differential equation for the relative phase between the master and the slave. This equation will let us investigate the effects of noise on the steady-state locking condition and transients of the locking process.

The next section presents the theory of semiconductor laser injection locking. The analysis is based on the rate equations and includes the effects of gain saturation, amplitude-phase coupling, and carrier dynamics. The analysis includes Langevin noise terms in the rate equations. It is also shown in this section, that one can obtain Adler's equation from the rate equations if the carrier dynamics are neglected. The important deterministic features of semiconductor laser locking is presented in Section III. These features include locking bandwidth and phase transients. Various effects due to the presence of noise are discussed in Section IV. Section V is a presentation of experimental results which show the time necessary to lock to semiconductor lasers. The dependence of the locking time on frequency detuning and locking bandwidth is

also shown. Section VI concludes the paper with a discussion of the importance of the results presented.

II. THEORY OF SEMICONDUCTOR LASER LOCKING

The interaction of the optical field with a lasing medium can be described by a coupled set of differential equations for electric field, the carrier density, and the polarizability [46]. However, the very short scattering times in the semiconductor cause the induced dipole moment to decay quickly. This allows one to adiabatically eliminate the polarizability from the set of equations. Therefore, one is left with three quantities, the amplitude and phase of the electric field, and the carrier density. Injection locking phenomena can be described using these three physical quantities if we include an additional electric field inside the cavity corresponding to the injected signal.

We can write the differential equations for the electric field and the carrier density of a semiconductor laser with injection as, [40], [26],

$$\frac{\partial \mathcal{E}_s}{\partial t} = \left(j\omega_s + \frac{1}{2} (\hat{G} - \gamma) \right) \mathcal{E}_s + \sqrt{\eta} f_d \mathcal{E}_m + \mathcal{F} \quad (1)$$

$$\frac{\partial N}{\partial t} = J - \frac{N}{\tau_s} - G |\mathcal{E}_s|^2 \quad (2)$$

where \hat{G} is the complex intensity gain per unit time, G is the real part of the gain, γ is the loss, τ_s is the spontaneous lifetime, \mathcal{F} is a Langevin noise term, N is the carrier density, J is the pump term, and ω_s is the slave free running steady-state frequency. The electrical field of the slave laser \mathcal{E}_s and the master laser \mathcal{E}_m can be expressed as

$$\mathcal{E}_s = E_s e^{j(\omega_s t + \phi_s(t))} \quad (3)$$

$$\mathcal{E}_m = E_m e^{j(\omega_m t + \phi_m(t))}. \quad (4)$$

The field amplitude, E_s , has been normalized such that $|E_s|^2$ is equal to the photon number S . The η parameter is used to correct the ratio of E_m/E_s . This correction factor is the product of η_m and η_r , where η_m represents the field overlap of the injected field and the laser mode field, and η_r is a correction due to the facet reflectivity. Assuming E_m and E_s are the field strengths outside the laser cavities, an expression can be derived for η_r in terms of the facet reflectivity,

$$\eta_r = \frac{(1 - R)^2}{R}. \quad (5)$$

The factor f_d in the electric field equation is the inverse of the round-trip time of the slave laser cavity. This corresponds to the longitudinal mode spacing and has a typical value of 125 GHz.

The Langevin noise term is assumed to be Markoffian [47] meaning that the random forces have no memory. This can be represented mathematically as

$$\langle \mathcal{F}(t) \mathcal{F}(t + \Delta t) \rangle = 2D\delta(\Delta t) \quad (6)$$

where D is the diffusion coefficient. The assumption that the system has no memory is adequate for semiconductor

lasers since the polarization relaxation time is on the order of 10^{-13} , which is negligible compared to the photon lifetime and carrier relaxation times [48]. The noise source in the carrier equation is neglected because it has been shown to be insignificant relative to the intensity and phase noise source [49].

The complex gain can be expressed as a Taylor expansion around the steady-state operating point [50]

$$\hat{G}(N, S) = G(N_h, S_0) + \frac{\partial G}{\partial N} (1 + j\alpha) \Delta N + \frac{\partial G}{\partial S} \Delta S \quad (7)$$

where

$$\Delta N = N - N_h \quad (8)$$

$$\Delta S = S - S_0 \quad (9)$$

and α is the linewidth enhancement factor. The last two equations basically point out that at steady state the laser operates with a carrier density equal to the threshold density and a photon number of S_0 . We include the effect of gain saturation by assuming the gain has a photon number dependence given by $G(1 - \kappa_i S)$. Therefore, $\partial_y G = -\kappa_i G$.

To reduce the number of parameters in the rate equations we adopted the following definitions:

$$\tau = \omega_r t \quad (10)$$

$$i = \frac{\Delta S}{S} = \frac{2\Delta E_s E_{s0}}{E_{s0}^2} = \frac{2\Delta E_s}{E_{s0}} \quad (11)$$

$$u = (\omega_m - \omega_s)t + (\phi_m(t) - \phi_s(t)) = \Delta\omega t - \Delta\phi \quad (12)$$

$$n = \frac{G_N \Delta N}{\omega_r} \quad (13)$$

where ω_r is the relaxation frequency given by [51]

$$\omega_r^2 = GG_N E_{s0}^2 = \frac{G_N E_{s0}^2}{\tau_p} \quad (14)$$

and $G_N = \partial G / \partial N$. Also, without loss of generality, E_{s0} is assumed to be real. Substituting (3) and (4) in (1) and (2), and introducing the normalized quantities one can obtain the final form of the injection locking rate equations:

$$\frac{\partial i}{\partial \tau} = n - \frac{\kappa_i E_{s0}^2}{\tau_p \omega_r} i + \frac{2f_d \sqrt{\eta} E_m}{\omega_r E_{s0}} \cos(u) + F_i \quad (15)$$

$$\frac{\partial \phi_s}{\partial \tau} = \frac{1}{2} \alpha n + \frac{f_d \sqrt{\eta} E_m}{\omega_r E_{s0}} \sin(u) + sF_{\phi_s} \quad (16)$$

$$\frac{\partial n}{\partial \tau} = -(1 - \kappa_n E_{s0}^2) i - \left(\frac{1}{\tau_s \omega_r} + \tau_p \omega_r \right) n. \quad (17)$$

In (15) we have neglected a contribution due to the average spontaneous emission. The Langevin noise terms, F_i and F_{ϕ_s} , are related to the real and imaginary parts of \mathcal{F} , respectively. The diffusion constants can be found either by a rigorous mathematical analysis [52], or by physical arguments as shown by Henry [48]. In any case, the re-

sults are $D_{SS} = RS$, $D_{\phi\phi} = R/(4S)$, and $D_{S\phi} = 0$, where S is the photon number and R is the spontaneous rate. Applying the normalizations used in this paper, we can write the noise sources of (15) and (16) as

$$F_i(\tau) = \frac{F_S(\tau/\omega_r)}{S\omega_r} \quad (18)$$

$$F_{\phi_s}(\tau) = \frac{F_\phi(\tau/\omega_r)}{\omega_r}. \quad (19)$$

Consider the D_{ii} diffusion constant. We can compute the value of this constant by writing

$$\begin{aligned} \langle F_i(0)F_i(\Delta\tau) \rangle &= \frac{1}{S^2\omega_r^2} \langle F_S(0)F_S(\Delta t/\omega_r) \rangle \\ &= \frac{2D_{SS}}{S^2\omega_r^2} \delta\left(\frac{\Delta t}{\omega_r}\right). \end{aligned} \quad (20)$$

We can use the scaling property of the delta function [53], $\delta(t/a) = |a|\delta(t)$ to write the normalized expression for the diffusion constants as

$$D_{ii} = \frac{R}{S\omega_r} \quad (21)$$

$$D_{\phi_s\phi_s} = \frac{R}{4S\omega_r}. \quad (22)$$

By adiabatically eliminating the amplitude and carrier variations from the normalized system of equations, it is possible to derive a single nonlinear differential equation for the phase ϕ_s with Langevin noise source F_s which includes amplitude-phase coupling. In Section III-A we will show that this adiabatic approximation is adequate for describing locking phenomena in the weak injection limit. This is because the phase transients (to be discussed in the next section) for weak enough injection last for times longer than $1/f_r$. When a laser is adiabatically perturbed (i.e., there is negligible change in the amplitude, phase and carriers in times less than $1/f_r$), there are no noticeable relaxation oscillations which means that the photon and carrier dynamics can be ignored when studying phase transients. Therefore, we can assume

$$\frac{\partial i}{\partial \tau}, \frac{\partial n}{\partial \tau} \ll i, n. \quad (23)$$

Also notice that the master laser is described by (15)–(17) if E_m is set to zero. Therefore, we can also derive a single equation for the master phase ϕ_m . The phase equations for the master and slave lasers are

$$\begin{aligned} \frac{\partial \phi_s}{\partial \tau} &= \sqrt{1 + (\alpha\beta)^2} \frac{f_d E_m}{\omega_r E_{s0}} \sin(\Delta\omega t + \Delta\phi(t)) \\ &\quad - \arctan(\alpha\beta) + F_s, \end{aligned} \quad (24)$$

$$\frac{\partial \phi_m}{\partial \tau} = F_m \quad (25)$$

where $\Delta\phi = \phi_m - \phi_s$, F_s and F_m are the Langevin noise terms and β is given by

$$\beta = \frac{1 - \kappa_n E_{s0}^2}{1 - (\kappa_n - \kappa_i) E_{s0}^2 + \frac{\kappa_i E_{s0}^2}{\tau_p \tau_s \omega_r^2}}. \quad (26)$$

The diffusion constants of the master and slave lasers in terms of the observed linewidth are

$$D_{mm} = \frac{\Delta\nu_m}{2f_r} \quad (27)$$

$$D_{SS} = \frac{\Delta\nu_s}{2f_r} \quad (28)$$

where $\Delta\nu_m$ and $\Delta\nu_s$ are the linewidths, both in units of Hertz. To obtain the diffusion constants, we neglected β since it was close to one, used the fact that the linewidths can be expressed by [48]

$$\Delta\nu = (1 + \alpha^2) \frac{R}{4S\pi}. \quad (29)$$

Now, we can obtain a single equation for the relative phase between the master and slave lasers by subtracting (24) from (25).

$$\frac{\partial \psi}{\partial \tau} = \frac{\Delta\omega}{\omega_r} - \frac{\Delta\omega_L}{\omega_r} \sin(\psi) + F_\psi \quad (30)$$

where

$$\Delta\omega_L = \sqrt{1 + (\alpha\beta)^2} \frac{f_d E_m}{E_{s0}} \quad (31)$$

$$\psi = \Delta\omega t + \Delta\phi - \arctan(\alpha\beta) = u - \arctan(\alpha\beta) \quad (32)$$

$$D_{\psi\psi} = \frac{1}{2f_r} (\Delta\nu_m + \Delta\nu_s). \quad (33)$$

The parameters κ_i and κ_n account for the possibility the gain saturation coefficient for the intensity equation may differ from that of the carrier equation.

III. DETERMINISTIC RESULTS

Except for the Langevin noise source, (30) is the same form as presented by Adler [2]. Directly from Adler's equation, it is possible to point out some characteristics about injection locking. First, in steady state,

$$\psi_{ss} = \arcsin\left(\frac{\Delta\omega}{\Delta\omega_L}\right). \quad (34)$$

Therefore, one immediately sees that there is a steady-state solution only if

$$|\Delta\omega| \leq \Delta\omega_L. \quad (35)$$

This expression [with $\Delta\omega_L$ given by (31)] is slightly different from previously reported theory of semiconductor laser locking. In particular, β is multiplying the linewidth

enhancement factor α . Formally, the inclusion of gain saturation results in the β factor, but typical values for β are close to 1. Since α is usually not known very accurately, the correction due to gain saturation can be ignored when calculating the locking bandwidth and steady state relative phase.

For the study of transients it is helpful to observe that (30) can be thought of as a zero mass object in a potential

$$V(\psi) = -\frac{\Delta\omega}{\omega_r} \psi - \frac{\Delta\omega_L}{\omega_r} \cos(\psi) \quad (36)$$

with a damping constant of one.

Plotting (36) will provide some insight into the locking process. Fig. 1 shows a potential function for which locking will occur. The variable ψ is equivalent to an overdamped particle in the potential. For example, ψ is the x coordinate of a marble on a surface like Fig 1 surrounded by a viscous fluid. If the marble is imagined on a surface shaped like Fig. 1 then it will settle into the bottom of one of the wells. Which well the marble settles into depends on the initial condition. For example, if at $\tau = 0$ the marble is at $\psi = -2$, then it will settle to the local minimum located at $\psi \approx 0.5$. As $\Delta\omega_L$ tends towards $\Delta\omega$ the depth of the potential well reduces, and when they are equal the potential no longer has local minima.

The transient nature of injection locking is of particular interest in this paper. Adler's equation can be directly integrated to provide a closed form solution of how the phase (frequency) changes as a function of time. As shown by Adler [2], the closed form solution is

$$\psi(\tau) = 2 \arctan \left[\frac{1}{k} + \frac{\sqrt{k^2 - 1}}{k} \cdot \tan \left(\frac{\Delta\omega_L(\tau - \tau_0)}{2\omega_r} \sqrt{k^2 - 1} \right) \right] \quad (37)$$

where

$$k = \frac{\Delta\omega}{\Delta\omega_L} \quad (38)$$

and τ_0 is used to fit to the initial relative phase condition. The normalized detuning parameter $|k|$ will be less than or equal to 1 if locking is possible. It is important to note that Adler's equation, and hence the analogy to describe the phase transient for Adler's solution, is valid only in the weak injection limit when neglecting relaxation oscillations.

Using (37) we can show that even if the laser is outside of the locking bandwidth the frequency of the slave is affected. Although the slave will not phase lock to the master, the frequency difference between the lasers will be pulled toward zero. As Adler showed [2], the frequency pulling can be expressed as

$$\Delta f_I = \frac{\Delta f \sqrt{k^2 - 1}}{k} \quad (39)$$

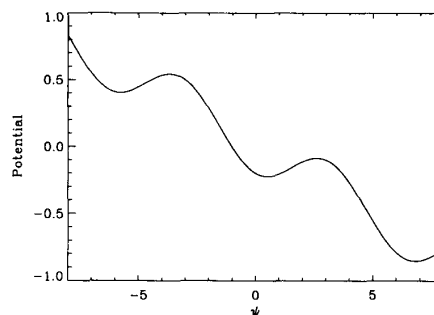


Fig. 1. Locking potential with $\omega_r/(2\pi) = 5$ GHz, $\Delta\omega/(2\pi) = 500$ MHz and $\Delta\omega_L/(2\pi) = 1$ GHz.

where Δf_I is the pulled frequency difference of the slave with injection and Δf is the free running frequency difference.

A. Numerical Integration of the Rate Equations without Langevin Noise Sources

In this section a discussion of the accuracy of Adler's solution will be presented. The means of determining the accuracy will be by comparing the output of the numerically integrated system of equations with Adler's solution. Euler's method was used to integrate the system. The only parameters that will be varied in this comparison will be the locking bandwidth $\Delta\omega_L/2\pi$ and the frequency detuning $\Delta\omega/2\pi$. We now will show the numerical results assuming the value of the locking bandwidth is 820 MHz and the frequency detuning is 200 MHz. The results are shown in Fig. 2(a) and (b). In Fig. 2(a), Adler's solution is shown as the dotted line, and clearly it has failed to include the relaxation ringing. Fig. 2(b) shows the normalized carrier density (dotted) and the normalized intensity (solid). We assumed a value of 4 for the linewidth enhancement factor, 5 GHz for the relaxation frequency, 125 GHz for the longitudinal mode spacing, 1.6 ps for the photon lifetime, 2.2 ns for the spontaneous lifetime, 1.18×10^{-2} for $\kappa_i E_{s0}^2$ and zero for $\kappa_n E_{s0}^2$. The details for the determination of these values has already been reported [54].

Next we show the effect of a nonzero rise time of the injected signal. This will primarily reduce the relaxation ringing of the system. Now consider Fig. 3 which is a plot of a numerical integration of the rate equations including a nonzero rise time for the injection signal. The injection signal used to create Fig. 3 has a 10 to 90% rise time of 0.2 ns. Notice the reduction of the amplitude of the relaxation oscillations as compared to Fig. 2. For a rise time of 0.2 ns, it is almost impossible to notice any ringing at all. This is not to surprising since 0.2 ns is the period of the 5 GHz relaxation frequency used in the integration and as stated earlier, if a laser is adiabatically perturbed (i.e., small changes in relative phase for times less than $1/f_r$) the relaxation oscillation amplitude is reduced tremendously.

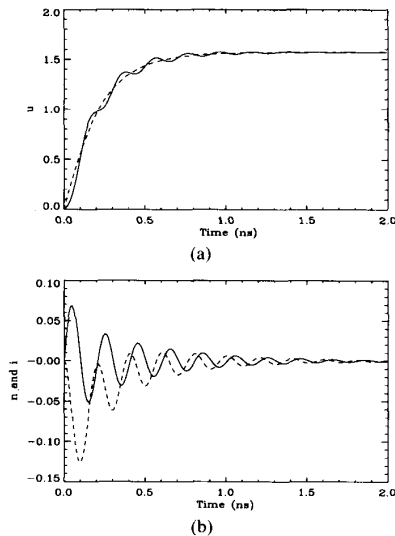


Fig. 2. Integration of the rate equations for $\Delta\omega_L/(2\pi) = 820$ MHz and $\Delta\omega/(2\pi) = 200$ MHz. In (a), u is the relative phase between the master and slave lasers, the dotted line is Adler's solution and the solid line obtained from integrating the rate equations. In (b), both plots are results of the numerical simulation of the rate equation. The dotted line is the normalized carrier density and the solid line is the normalized intensity.

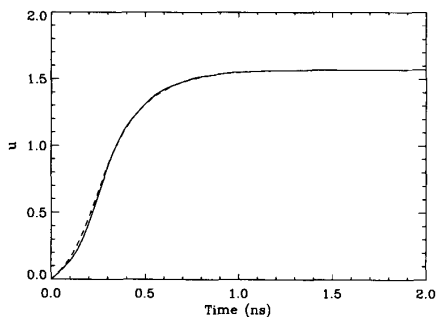


Fig. 3. Effect of nonzero rise time of injection signal on phase transients. The solid line is the integration of the rate equations and the dotted line is Adler's solution. $\Delta\omega_L/(2\pi) = 820$ MHz and $\Delta\omega/(2\pi) = 200$ MHz. The rise time of the injected signal was 3.5 ns.

IV. NOISE EFFECTS ON TRANSIENT PHENOMENA OF INJECTION LOCKED SEMICONDUCTOR LASERS

For the solutions presented in the last section, the three rate equations were assumed to be deterministic, therefore, at steady state the laser would remain unchanged with time. However, if the laser is in steady state and a spontaneous emission event occurs, then the output power of the laser changes slightly from the deterministic steady-state value. The laser attempts to return to the steady state via damped oscillations at the relaxation frequency. Since spontaneous emission is unavoidable, and also since the laser has a natural resonance at the relaxation frequency, the power spectrum of the relative intensity noise, RIN, will have a local maximum at the relaxation frequency. The phase of the laser field is also changed slightly when a spontaneous event occurs. This is because a sponta-

neously created photon, unlike a stimulated one, has an arbitrary phase and the amplitude fluctuations couple to the phase fluctuations through the α factor.

In the remainder of this section we will discuss the effects of noise on injection locked semiconductor lasers. We will show that there are a few properties of injection locking in which noise plays an important role. In Section IV-A the Fokker-Planck equation is used to describe phase transients. In Section IV-B a discussion of phase transients which are most influenced by noise is presented. It is shown that for certain initial conditions, the time to lock is tremendously reduced as compared to a deterministic analysis. In Section IV-C we will use the Fokker-Planck equation to show the effects of noise on the steady-state locking condition. Then in Section IV-D we will address the steady-state condition using a power spectral density analysis. This analysis will allow us to see the effects of a finite detector bandwidth on the measured phase statistics. In Section IV-E we point out another difference between the deterministic development of the last chapter and the analysis including noise. We will discuss the fact that there is a probability for the locked lasers to unlock and the relative phase to jump 2π .

A. Fokker-Planck Analysis of Phase Transients

Using the stochastic differential equation (30) derived in Section II, we will now analyze some of the effects that noise has on injection locking. It is known that there is a correspondence between a stochastic differential equation of the form presented in Section II and the Fokker-Planck equation [55]. The equivalent Fokker-Planck equation corresponding to (30) has the following form:

$$\frac{\partial f(\psi, \tau)}{\partial \tau} = -\frac{\partial}{\partial \psi} \left[\left(\frac{\Delta\omega}{\omega_r} - \frac{\Delta\omega_L}{\omega_r} \sin(\psi) \right) f(\psi, \tau) \right] + D_{\psi\psi} \frac{\partial^2}{\partial \psi^2} f(\psi, \tau). \quad (40)$$

The Fokker-Planck solution describes the time evolution of the probability density function $f(\psi, \tau)$. That is, given an initial condition, ψ_0 and τ_0 , the solution can be expressed mathematically as

$$f(\psi, \tau) = p(\psi, \tau | \psi_0, \tau_0) \quad (41)$$

where $p(a|b)$ is the conditional probability density. In our application we will consider the initial condition to be a uniformly distributed probability density function over 2π radians. This is due to the fact that we do not know the relative phase between the master and the slave at the instant the injected signal is incident on the slave.

It is instructive to look at some plots of the Fokker-Planck solution. The following plots are for a locking bandwidth of 500 MHz, a frequency detuning of 200 MHz and a sum of the linewidths of 20 MHz. Fig. 4 shows a plot of the initial condition. The plot shows both the probability density function (solid) and the potential function (dotted). The uniform distribution is positioned such that

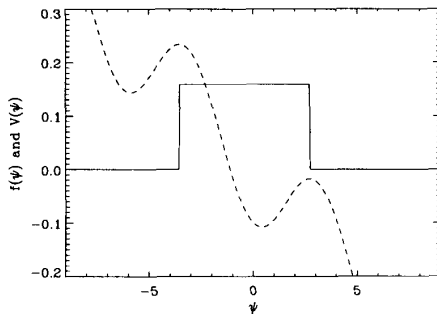


Fig. 4. Initial condition for the Fokker-Planck equation. The dotted line is the potential corresponding to a locking bandwidth of 500 MHz, a frequency detuning of 200 MHz, and a relaxation frequency of 5 GHz. The solid line is the probability density function of the relative phase between the master and slave laser.

much of the distribution will converge to the local minimum located near zero. Fig. 5 shows the probability distribution function at $t = 0.56$ ns. The density function has already begun to take the form of a Gaussian. The potential plotted in the figure is the same potential as shown in Fig. 4. It appears different because the y axis is scaled differently. The Gaussian is roughly centered around the minimum of the potential as expected. In Fig. 6 we see how the variance changes with time. This plot assumed the same conditions as before, that is a locking bandwidth of 500 MHz and a frequency detuning of 200 MHz. As one can see, the variance is close to the steady-state value after about 2 ns. This can be understood by recalling that the deterministic phase transients discussed in Section II were shown to have time constants of approximately $1/\Delta\omega_L$. Regardless of the initial relative phase, all the phase transients will be near the steady state in about 2 ns for a locking bandwidth of 500 MHz. Therefore, at that point in time only the noise is contributing to the distribution of the phase (and the variance).

B. Phase Transients Equivalent to the Decay of an Unstable Equilibrium

Many applications which utilize the phase-locked condition, such as phase modulation or frequency shift keying, have bandwidths which are limited by the time it takes to achieve locking. Many features of the locking process can be understood by examining the potential of the relative phase equation. In Fig. 4 the dotted line is a plot of the potential for a locking bandwidth of 500 MHz and a frequency detuning of 200 MHz. Consider an initial relative phase distribution which is a delta function not near a relative maximum of the potential. In this case the phase will move towards a local minimum and settle to a steady state. Now, consider the special case where the initial relative phase is at the peak of one of the local maximums of the potential. In this situation, the phase is in an unstable equilibrium. However, the phase noise would move the phase away from this equilibrium. The question that we would like to address in this section is the mean time it takes for the value of ψ to move away from the maxi-

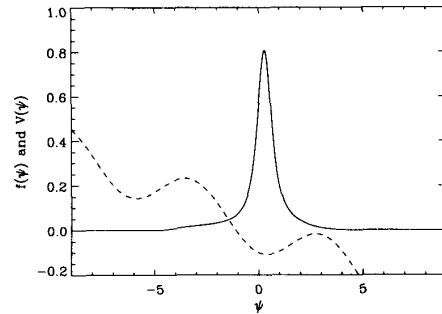


Fig. 5. Probability density function of the relative phase at $t = 0.56$ ns. The laser parameters are the same as that of Fig. 4.

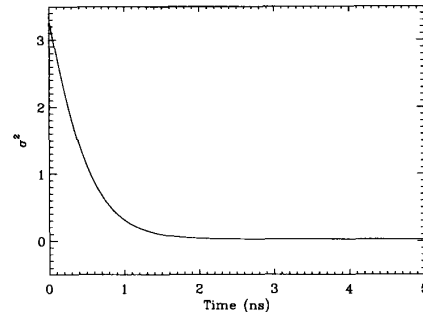


Fig. 6. Relative phase variance as a function of time. The laser parameters are the same as that of Fig. 4.

um to a position where the noise has little influence on the trajectory. If we could determine this mean time, then we could calculate the total locking time since we can use the deterministic solution from Section III to describe the remainder of the trajectory of ψ up to the point where it is near the local minimum of the potential. Fig. 7 shows three plots of the numerical integration of (30), each with different levels of noise. The noise level is determined by the sum of the linewidths of the free running master and slave lasers. In the figure, the three different total linewidths are shown, namely 20, 2, and 0.2 MHz. Clearly, the narrower linewidths lead to a larger transit time.

The statistics of the transit time away from an unstable equilibrium point has been addressed theoretically by a few different groups [56]–[59]. In particular, the work of Haake *et al.* [57] is quite general, thus it is straight forward to apply their results to our problem. They showed that if one has a stochastic differential equation of the form

$$\frac{\partial S(T)}{\partial t} = S(t) + F(t) \quad (42)$$

where $F(t)$ is a Langevin noise term with a diffusion constant D , then, if one starts out precisely at the point of unstable equilibrium, the mean time to move a distance M away from the initial point is given by

$$\hat{t} = \frac{1}{2} \left[\ln \left(\frac{M^2}{2D} \right) + \gamma + 2 \ln(2) \right] \quad (43)$$

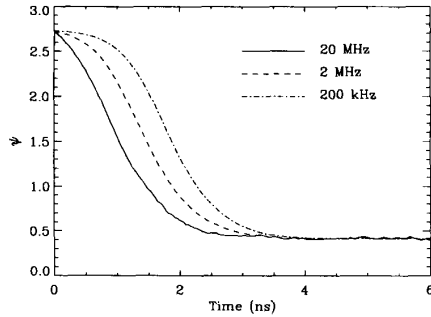


Fig. 7. Effect of linewidth on transit time away from a potential maximum. The locking bandwidth was 500 MHz and the frequency detuning was 200 MHz.

where γ is Euler's constant and is approximately 0.5772, and the variance of \hat{t} is given by

$$\sigma^2 = \frac{\pi^2}{2}. \quad (44)$$

The last two equations are valid given that

$$1 \ll \frac{M^2}{D}. \quad (45)$$

The condition just shown basically states that the distance M must be large enough such that the influence of the noise is small compared to the deterministic contribution.

We now will cast (30) into the form of (42) so we can make use of Haake's *et al.* results. The resulting mean time is given by

$$\hat{t} = \frac{1}{4\pi\Delta f_L \sqrt{1-k^2}} \left[\ln \left(\frac{M^2 \Delta f_L \sqrt{1-k^2}}{\Delta\nu_m + \Delta\nu_s} \right) + \gamma + 2 \ln(2) \right] \quad (46)$$

where t is in units of seconds. Using (44) we obtain the variance,

$$\sigma^2 = \frac{1}{8\Delta f_L (1-k^2)}. \quad (47)$$

In Fig. 7 we showed how the mean time varied with the sum of the linewidths of the lasers. We will now compare the plots to the theoretical expression of (46) to see how closely they match. The position where each plot crosses the $y = 2.0$ line represents the mean time to move a distance of $\pi - \arcsin(\Delta\omega/\Delta\omega_L) - 2.0 \approx 0.73$, therefore, the value of M to use in (46) is 0.73. Table I shows a comparison of the theoretical and numerical results. Notice how the accuracy of the numerical results improve as the total linewidth is reduced. This can be explained by noting that as the linewidths are reduced the diffusion constant is also reduced. The reduction of the diffusion constant means that the condition shown in (45) is more easily satisfied, thus the improved results.

It has been shown that noise does have an important effect on the time it takes two lasers to lock. However,

TABLE I
COMPARISON OF THEORETICAL AND NUMERICAL TRANSIT TIMES FROM AN UNSTABLE EQUILIBRIUM.

$\Delta\nu_m + \Delta\nu_s$ (MHz)	Theory (ns)	Numerical (ns)	% error
20.0	0.776	0.714	-8.0%
2.00	1.175	1.126	-4.2%
0.20	1.575	1.534	-2.6%

the relative influence that the noise has on the transit time is strongly dependent on the initial relative phase between the two lasers. If the initial relative phase is the location of a local maximum of the potential, then we now know that the noise is essential to obtain the correct locking time. Equation (45) provides us with an expression by which to determine the influence of the noise. If (45) is not satisfied (when we use $M = \psi(0)$), then the effect of the noise is important. On the other hand, if the initial relative phase is such that (45) is easily satisfied, then we can use the deterministic solution of Section II. The overall time to lock can be determined by using the deterministic analysis for initial conditions away from the maximum of the potential, and (46) for the initial condition near the maximum.

There has been some previous work dealing with the transit time statistics for semiconductor lasers. In particular, some groups have discussed the turn-on time delay of a semiconductor laser below threshold which is subjected to a step of the injection current which pushes the laser above threshold [60], [61]. This is analogous to the problem of injection locking since far below threshold, the nonzero intensity is due to spontaneous emission perturbing the intensity from the deterministic steady-state value of zero. After the step in the injection current, the potential changes shape becoming a fourth-order polynomial with a local maximum at zero. As soon as this second potential is developed, the intensity is still at (or very near) zero. Therefore, we see that the laser will begin to lase by being perturbed off of the unstable equilibrium point. In general, the turn-on phenomenon in semiconductor lasers requires the consideration of the carrier dynamics, and in fact these earlier papers include this effect. It should be noted again that we have adiabatically eliminated the carrier dynamics from the problem to obtain the stochastic differential equation presented earlier in this chapter. We justify this by considering the weak injection limit which has been shown not to depend much on the carrier dynamics. If the effect of the carrier dynamics was included, the potential would be a more complex (three-dimensional) surface, and it would develop over a nonzero time. The time for the potential to settle to a steady state would be on the same order as the damping of the relaxation ringing. We used a damping constant, $\Gamma_r = 9.5 \times 10^9 \text{ s}^{-1}$, which means the damping time, $1/\Gamma_r$, is less than a nanosecond. However, regardless of how the potential is developed, it is still possible that the relative phase may be in a location of an unstable equilibrium point. Therefore, the analysis presented in this sec-

tion would be valid for the time necessary to fall off of the unstable point.

In short, the analysis of this section dealing with time transients shows that the deterministic solution is inadequate to describe the time transients for all initial conditions. In fact, the analysis presented here provides a significant improvement over the deterministic model which predicts an infinite fall time of the unstable equilibrium point. Including the carrier dynamics to the time to lock calculation would be a higher order correction to the analysis presented here.

C. Steady-State Locking Condition using Fokker-Planck Analysis

The Fokker-Planck differential equation will allow us to discuss the salient features of injection locked semiconductor lasers including the effects of noise. It is interesting to observe the difference between the steady-state solution derived in Section III with that of the Fokker-Planck equation. In section III, we used a potential to help describe both locking bandwidth and locking transients for the weak injection case. We recall that the steady-state value of ψ was determined by the position of a local minimum of the potential plotted in Fig. 1. It is clear from this figure and from the analysis that the steady-state value of ψ approaches a constant value. This is equivalent to a probability density function in the form of a Dirac delta function. This conclusion is only valid in the assumption that there is no noise in the system. The Fokker-Planck steady-state solution is therefore a much more accurate account of the locked state [42].

It is important to realize that the injection locking potential has no true steady state. This can be seen by considering the potential shown in Fig. 1 in Section III. If the value of the phase ψ is at a minimum of the potential, we know that there is a finite probability for the noise of the system to perturb the phase such that it escapes over the potential barrier. After the escape over the barrier, the phase settles into the new local minimum. Because of the shape of the potential shown in Fig. 1, the mean value of the phase will increase with time. That is, the phase is more likely to escape over the right barrier of any local minimum since it is smaller than the left barrier. Therefore, we see that the probability distribution function will never have a zero time derivative. This problem is studied in more detail in Section IV-E.

If the mean escape time over a potential barrier is very large, then the time derivative of the probability distribution is small and the steady-state Fokker-Planck equation can be expressed as

$$f(\psi) = c_0 \exp\left(\frac{-V(\psi)}{D_{\psi\psi}}\right) \quad (48)$$

where c_0 is a normalization constant and $V(\psi)$ is the injection locking potential as discussed in the previous section. This is accurate for times much smaller than the mean escape time. It will be shown in this section that the

mean escape time is enormous for typical values of the normalized detuning parameter k . In fact, for a frequency detuning of 200 MHz and a locking bandwidth of 500 MHz, we have calculated the escape time to be 10^{11} s.

Expanding this solution around the minimum of the potential we obtain a Gaussian probability density given by

$$f(\psi) = c_1 \exp\left(-\frac{\Delta\omega_L \sqrt{1-k^2}}{2\pi(\Delta\nu_m + \Delta\nu_s)} \Delta\psi^2\right) \quad (49)$$

where c_1 is a normalization constant. This form of the solution is useful for providing insight into the effect of noise on the locked state. This probability density function shows all the characteristics one would expect from known results of the steady-state noise characteristics in injection locked lasers [39], [40].

Looking at the exponent of (49) we see that as the linewidths of the lasers approach zero, the probability density becomes a delta function. This is not surprising since letting the linewidths approach zero is equivalent to ignoring the noise of the system and we already pointed out that without noise the probability density function is a delta function. Next, consider the effect of k approaching one. The slope of the potential around the minimum is reduced as k approaches one. This has a direct effect on the width of the probability density function. As (49) shows, as k approaches one, the variance of the probability density function increases. A very simple physical analogy showing this trend is shown in Fig. 8. As the marble is perturbed by a random noise force (spontaneous emission), the kinetic energy is converted to potential energy as the marble travels up the side of the potential. At the point where the potential energy equals the original kinetic energy the marble stops and returns to the minimum. For values of k closer to one the marble must travel further in the ψ direction before it stops we expect a higher probability to find the marble further from the minimum as predicted by (49).

The last term in (49) to be considered is $\Delta\omega_L$. We see that as the locking bandwidth, $\Delta\omega_L$ increases the width of the probability density function decreases. This can be understood by considering the transients of the ψ variable as discussed in Section III. The locking transient is roughly proportional to the inverse of the locking bandwidth. Let's consider how this effects the marble analogy. In the limit as the bandwidth approaches infinity the time it takes for the marble to return to the minimum goes to zero. Therefore, when a random noise event perturbs the marble from the minimum, it will immediately return before the next random event. Now, as the locking bandwidth is reduced, we see that the marble will take some finite amount of time to return to the minimum. During this return trip, the marble could be perturbed by another random noise event. If the time to return to the minimum is long enough, then the marble could experience many perturbations which can move it further from the minimum than any single noise event could. Therefore, as the locking bandwidth is reduced it is reasonable to expect a

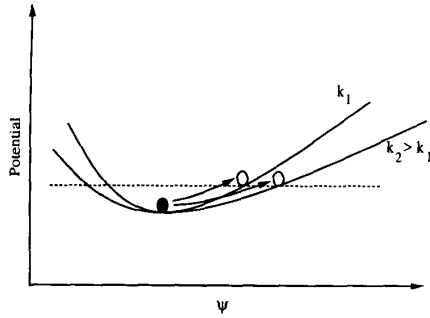


Fig. 8. Effect of increasing k on displacement from steady state.

higher probability to find the marble further from the minimum of the potential. It seems that (49) is an acceptable expression describing the probability density function.

D. Steady-State Locking Condition Using Power Spectral Density Analysis

In the last section we derived an expression for the probability density function for the relative phase between the master and slave injection locked lasers. We showed that the form of the distribution was a Gaussian with a variance of

$$\sigma^2 = \frac{\Delta\nu_m + \Delta\nu_s}{2\Delta f_L \sqrt{1 - k^2}}. \quad (50)$$

For a frequency detuning of 200 MHz, locking bandwidth of 500 MHz, and a sum of linewidths of 20 MHz, the standard deviation is approximately 8° . However, the variance (standard deviation) is directly affected by the detection process. It will be shown that the observed variance of the relative phase can be reduced by using a realistic phase detector, that is one with a finite bandwidth.

It will be easier to derive an expression for the effect of the detector bandwidth on the variance of the relative phase of the lasers if we use a power spectral density approach. The variance of a process can be expressed as the integral over all frequencies of the power spectrum of the process [62]. We carried out the calculation and the result is the same as that of the Fokker-Planck analysis. However, the advantage of the power spectrum approach is that it allows us to consider the effects of a limited bandwidth detector by reducing the limits of integration in the variance calculation. Linearizing Adler's equation around steady state, the power spectrum can be expressed as

$$S_{\Delta\psi} = \frac{2\pi(\Delta\nu_m + \Delta\nu_s)}{\omega^2 + \gamma^2} \quad (51)$$

where $\gamma = \Delta\omega_L \sqrt{1 - k^2}$. We can calculate the variance by using the following [62]

$$\langle \Delta\psi^2 \rangle = \frac{1}{2\pi} \int_{-2\pi B}^{2\pi B} \frac{2\pi(\Delta\nu_m + \Delta\nu_s)}{\omega^2 + \gamma^2} d\omega \quad (52)$$

where B is the phase detector bandwidth in Hertz. The integral has a solution of

$$\langle \Delta\psi_B^2 \rangle = \frac{\Delta\nu_m + \Delta\nu_s}{\pi\Delta f_L \sqrt{1 - k^2}} \arctan \left(\frac{B}{\Delta f_L \sqrt{1 - k^2}} \right). \quad (53)$$

Evaluating the last equation as B approaches infinity gives the same result that was obtained using the Fokker-Planck analysis. However, by changing the limits of integration it is possible to obtain the effects of limited detection bandwidth on the variance. The infinite bandwidth standard deviation of about 8° is reduced to about 0.3 degrees with a detector bandwidth of 1 MHz. Equation (51) also represents the phase noise of the beat note between the master and the slave. From the form of (51) it follows that the beat note consists of a sharp spectral line riding on a flat noise background suppressed by $S_{\Delta\psi}(0)$.

E. Mean Passage Time in a General Potential

There is another interesting difference between the analysis of injection locking in the presence of noise and the deterministic analysis of Section III. It was shown that if

$$\left| \frac{\Delta\omega}{\Delta\omega_L} \right| \leq 1 \quad (54)$$

the lasers would lock together. This locked condition is maintained for as long as the above condition is maintained. However, it is possible for the relative phase to move to adjacent minima by *jumping* over the potential barriers. If the relative phase is not held constant, then the lasers are not locked, at least as defined in the deterministic analysis. However, the conditions for locking can be slightly modified to define that two lasers are locked if the relative phase doesn't jump over a barrier in some length of time.

A general development of transit times in a potential has been presented by Gardiner [55]. The result was a double integral which can be used to calculate the mean time to pass from point a to point b in a given potential. The expression is

$$T(a \rightarrow b) = \frac{1}{D} \int_a^b dy \exp(V(y)/D) \cdot \int_{-\infty}^y \exp(-V(z)/D) dz \quad (55)$$

where, as before, D is the diffusion constant of the Langevin noise term and $V(y)$ is the potential. The double integral is easy to solve in the limit of no injection since the potential reduces to

$$V(y) = \frac{\Delta\omega}{\omega_r} y. \quad (56)$$

The result of the integration is

$$T(a \rightarrow b) = \frac{b - a}{\Delta\omega}. \quad (57)$$

This is expected since in the case of no injection the master and slave lasers are separated in frequency by $\Delta\omega/(2\pi)$. Therefore, the relative phase between the two lasers changes at a rate of $\Delta\omega$ radians per second. Thus the time necessary to pass through $(b - a)$ radians is as given in the last equation.

Equation (55) was integrated numerically and the result is shown as the dotted line in Fig. 9. The escape time plotted in this figure represents the mean time it takes for the relative phase to pass from its present location (near a local minimum) to an adjacent local minimum. There are 2π radians separating the adjacent local minima, therefore, the inverse of the time plotted represents the relative frequency difference between the master and slave lasers.

Adler's theory predicts frequency pulling outside of the locking bandwidth $|k| > 1$ and this pulling was expressed in (39). Looking at Fig. 9, the solid line, for values of k greater than 1, is a plot of the inverse of the pulling (39). Equation (39) is equal to zero for k equal to one, therefore, the plot of the inverse has a singularity at this point. However, we see that the dotted line, representing the pulling including the noise of the lasers is finite at k equal to one. This is because the random noise forces can result in perturbing the relative phase, whereas the deterministic solution shows the locking occurs at this point. The major point to make about the difference is that Adler's theory predicts an absolute transition to lock, namely when $|k|$ is less than or equal to one, whereas the analysis including noise shows that the transition to the locked state is a matter of definition. It is clear, unlike the analysis of Section III, that the two lasers are theoretically never completely phase locked. Not only does the steady state phase continually experience perturbations away from the local minimum of the potential, but it also experiences 2π radian phase jumps when it escapes of the potential barrier.

Following Gardiner's [55] treatment, we can obtain approximate results for the escape time for $k < 1$. Gardiner shows that if near the minimum of the potential (point a) the potential can be written as

$$V(\psi) \approx V(a) + \frac{1}{2} \left(\frac{\psi - a}{\alpha} \right)^2 \quad (58)$$

and near the peak of the potential barrier it can be written as

$$V(\psi) \approx V(b) - \frac{1}{2} \left(\frac{\psi - b}{\delta} \right)^2 \quad (59)$$

then (55) could be solved approximately as

$$T \approx 2\alpha\delta\pi \exp \left(\frac{V(b) - V(a)}{D} \right). \quad (60)$$

This approximate solution assumes that the potential barrier is sharply peaked at b and the diffusion constant is small. Therefore, we can conclude that this approximation will break down as the normalized detuning constant

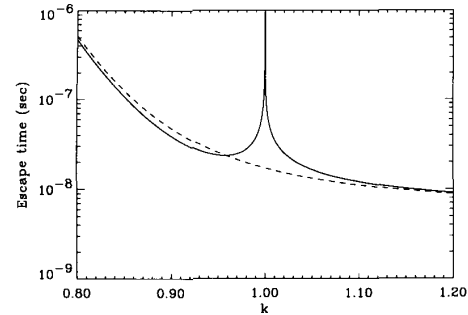


Fig. 9. Numerical evaluation of the mean escape time integral. Recall that k is defined as the locking bandwidth divided by the frequency detuning. The frequency detuning used in this figure was 200 MHz. The solid line for values of $k > 1$ is the inverse of Adler's frequency pulling equation. The solid line for values of $k < 1$ is Arrhenius formula.

approaches one, since at this point there is no potential barrier at all.

Gardiner indicates that (60) is the classical Arrhenius formula of chemical reaction theory. Also, as Risken points out, it is approximately the same as Kramer's escape time over a potential barrier [63]. Expanding the potential near the local minimum and the local maximum, we can rewrite (60) for the problem of escape time of injection locked semiconductor lasers. The result is

$$t = \frac{1}{\Delta f_L \sqrt{1 - k^2}} \cdot \exp \left(\frac{2\Delta f (2 \arcsin(k) - \pi) + 4\Delta f_L \sqrt{1 - k^2}}{\Delta\nu_m + \Delta\nu_s} \right). \quad (61)$$

A plot of (61) is shown in Fig. 9 as the solid line for values of k less than one. As can be seen in the figure, (61) is a good approximation for values of k which are not very close to one.

There is a close relationship between the mean escape time and the steady-state relative phase probability density function. There is a finite probability that the relative phase will be located past a potential barrier separating two local minima of the locking potential. Intuitively, once the relative phase *tunnels* through the potential barrier, it settles into the adjacent local minimum. The knowledge of the probability density function alone will not allow one to calculate the mean escape time. However, as just shown, the Fokker-Planck equation allows us to show the relationship between the probability density function and the escape time.

In Fig. 10 one can see how quickly the mean escape time grows. One sees that for a value of $k = 0.5$ the mean escape time is on the order of 1000. This illustrates the fact that effects of noise are negligible for values of k less than 0.5. The useful range of the locking bandwidth will depend upon specific applications.

The phase jumping described by (61) is analogous to the mode jumping observed in external cavity lasers as discussed by Mork *et al.* [64].

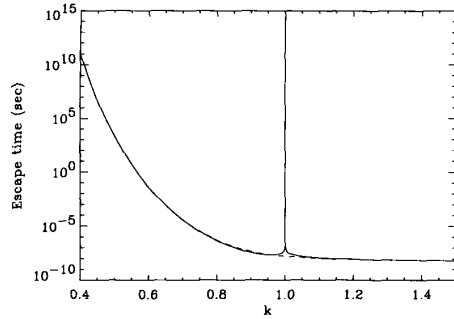


Fig. 10. Expanded view of the mean escape time. The laser parameters are the same as that of Fig. 9.

V. EXPERIMENTAL MEASUREMENTS OF LOCKING PROPERTIES

To our knowledge, no experiment has been reported on the locking time in semiconductor lasers. In this section we will present the results of our experiment which measures the time to lock of GaAlAs Fabry-Perot laser diodes. We will show that the results are consistent with the model developed in the previous sections.

A. Experimental Arrangement for Measuring Mean Locking Time

The schematic of the experiment is shown in Fig. 11. The slave is isolated (70 dB) from the input of the fiber to prevent reflection feedback as well as injection from the slave. A polarization controller in one of the optical fibers is used to match the polarization of the two fibers before beating the signals in a 3 dB fiber coupler. One output of the coupler was detected and displayed on a spectrum analyzer. The other output passed through a static Fabry-Perot interferometer and was displayed on an oscilloscope.

In this experiment, we utilized the fact that a slave laser could be locked to a sideband of a modulated master laser. The master laser was modulated with a 5 GHz pulse modulated microwave signal. The pulse modulation frequency was on the order of 3 to 4 MHz. We operated the slave laser such that the lasing frequency was very close to one of the sidebands of the master. This was accomplished by blocking the injection signal and observing the beat note on the spectrum analyzer. To understand the experiment, assume that the slave is lasing at a frequency 200 MHz away from the frequency of the first-order sideband of the master. During the time that the master is not being modulated (i.e., no sidebands) the slave does not lock since there is no signal present. This assumes that the locking bandwidth is much less than 5 GHz so that the slave does not try to lock to the center carrier of the master laser. Then the master is modulated (i.e., sidebands appear) and the slave laser frequency changes since the laser is locking to the sideband. Therefore, the time to lock could be measured by observing this frequency change.

We used a Fabry-Perot interferometer as a frequency discriminator to monitor the frequency change of the slave

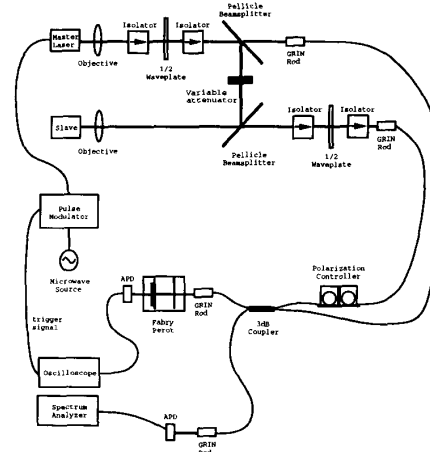


Fig. 11. Experimental arrangement used to measure mean time to lock.

laser during the locking transient. The Fabry-Perot was operated in a static mode such that the frequency of the free running slave laser was near a cavity resonance as shown in Fig. 12. Then as the frequency changes due to the influence of the injected signal, the frequency change is converted to an intensity change because of the characteristics of the Fabry-Perot resonance. We can monitor this intensity modulation on an oscilloscope which is triggered by the pulse modulator.

There are several points to consider about this technique. The transient of the slave laser is directly related to the initial value of the relative phase between the master and the slave. Since we did not have information about the initial phase condition, we performed an ensemble average by averaging many traces on the oscilloscope. Also, the characteristics of the Fabry-Perot, that is the free spectral range and the finesse, can have a major effect on the results of the experiment. We derived an expression for the transient response of a Fabry-Perot cavity. The intensity output can be written as

$$I \propto \frac{1}{2} - \mathcal{F}\tau\Delta f(t) + E \quad (62)$$

where τ is the round-trip time of the cavity, \mathcal{F} is the finesse, and E is an error term which shows the deviation of the Fabry-Perot from a perfect frequency discriminator. We simulated a Fabry-Perot cavity with a finesse of 100 and a mirror spacing of approximately 0.7 mm and found the E was negligible for the frequency transients resulting from injection locking considered in this paper.

B. Results of Mean Time to Lock Measurement

We will discuss the procedures used to measure the effect of operating condition on the mean time to lock. We will begin the section by discussing the experimental determination of the frequency detuning and the locking bandwidth. Then we will discuss frequency overshoot which was first noticed in the output of the numerical evaluation of the model and then in the laboratory. We will then present experimental results showing the de-

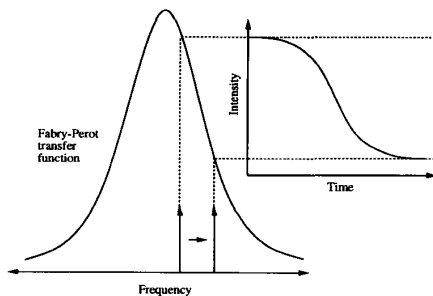


Fig. 12. Use of static Fabry-Perot to monitor slave laser frequency transient.

pendence of the mean locking transient on the frequency detuning. Similarly, experimental results showing the mean transient dependence on the injection level are also presented.

1) *Experimental measurements of frequency detuning and locking bandwidth:* We would like to point out some important points about the frequency detuning and locking bandwidth estimates used in the following sections. The fit of the theoretical plots to the experiment results is very dependent on one's confidence in these two parameters.

The locking bandwidth of this experiment was estimated by observing the beat note on the spectrum analyzer. As the frequency detuning of the two lasers was reduced by controlling the current of the slave laser we observed the beat note frequency approach zero. The deterministic model predicts that there is a distinct transition to the locked condition. However, as shown in the last section, the noise of the system causes the phase of the two lasers to change. Therefore, even though there are local minima in the potential, one can still observe a beat note on a spectrum analyzer. Experimentally this means it is difficult to exactly determine the locking bandwidth. Also, the beat note before locking had a full width half maximum of 20 MHz which limited our ability to obtain frequencies from the spectrum analyzer.

The frequency detuning of the two lasers is more difficult to obtain in our experiment. In a more simple locking experiment where the master laser is unmodulated, it is much easier to obtain the detuning. One only needs to block the injected signal to obtain the free running frequency detuning on a spectrum analyzer. However, our situation is more complicated. The model we are using contains the necessary information to describe locking between a single master frequency and a single slave frequency. The experiment we carried out involved locking the slave to a sideband of a modulated master laser. Therefore, the presence of the carrier will have an effect on the slave which is not accounted for in the model. We attempted to measure the effect of the carrier by placing the slave frequency 1.5 GHz less than the sideband frequency of the master. Since we have a 5 GHz modulating frequency, the slave is operating a frequency of $f_m + 3.5$ GHz, where f_m is the frequency of the master carrier.

Now, when we unblocked the injection signal we noticed that the slave frequency pulls toward the carrier. If the effect of carrier was negligibly small, we would expect the slave frequency to pull slightly towards the sideband (assuming the locking bandwidth were much smaller than 1.5 GHz). Therefore, we had to compensate for the pulling due to the carrier when estimating the frequency detuning. We measured the frequency pulling towards the carrier frequency to be on the order of 150 MHz for the experiments just discussed. This means that when we observe a frequency detuning of 50 MHz then the actual detuning would be approximately 200 MHz. There is some uncertainty in the estimate because we know that the pulling toward the carrier is competing with the pulling of the sideband.

2) *Frequency overshoot:* We have determined that the frequency overshoot is due to the nonzero rise time of the injected signal. To assist in the understanding of this phenomenon, consider the case of zero rise time. In Fig. 13(a) the phase transients for different initial conditions are shown. The frequency detuning to obtain these numerical results was assumed to be 100 MHz and the locking bandwidth was assumed to be 500 MHz. The mean frequency transient can be obtained by averaging the derivatives of the phase transients. Now consider a nonzero rise time as shown in Fig. 13(b). This figure shows phase transients for different initial conditions assuming a 3.5 ns rise time on the injected signal. We can describe the difference between this plot and the plot of Fig. 13(a) by using the potential description of locking. The minimum of the potential (after the injection reaches full strength) is located at approximately 0.2. However, initially, the injection level is zero, and the potential is just a straight line with negative slope. The derivatives of all the transients are equal to $(2\pi) 100 \times 10^6$ radians per second since this is the free running frequency difference. As the injected signal increases the potential changes. At a particular point in time, the potential obtains local minima. At this point we know (deterministically) that the phase transients immediately head for a local minimum. Consider the phase transient with the initial condition near -4 . As the phase increases the potential is simultaneously changing. However, before it reaches the value of 0.2 the potential already has a local minimum and the phase comes to rest. Next, consider the transient which has an initial condition near 2. The phase is increasing at the same time as the potential is changing, however, when the minimum appears the rate at which the phase is changing slows. Eventually, the phase reverses direction and travels back towards the minimum. The process of slowing and reversing direction delays the trajectory significantly. Looking at Fig. 13(b) we see that the presence of the delayed transients which started near 2 result in a mean frequency (derivative of the phase) which is negative for times roughly between 4 and 5 ns. This causes the mean frequency to exhibit overshoot.

We have experimentally observed the frequency overshoot as shown in Fig. 14. The experimental frequency

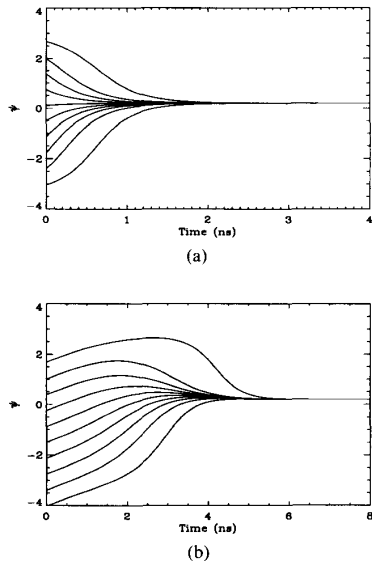


Fig. 13. (a) shows phase transients for different initial conditions with a zero second rise time on the injected signal. The locking bandwidth was 500 MHz and the frequency detuning was 200 MHz. (b) shows phase transients for different initial conditions but assumes a 3.5 ns rise time on the injected signal.

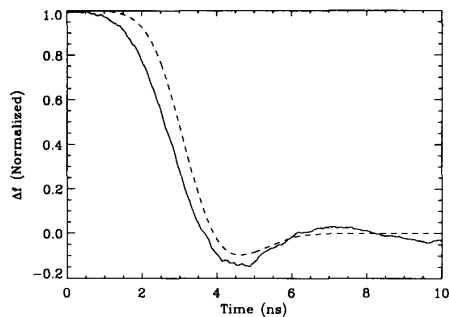


Fig. 14. Comparison of Fokker-Planck and experimental results showing frequency overshoot. The dotted line is the Fokker-Planck solution and the solid line is the averaged and smoothed data. The locking bandwidth was approximately 450 MHz and the frequency detuning was 100 MHz.

detuning and locking bandwidth was 100 and 450 MHz, respectively. Recall that the frequency detuning is defined as the master frequency minus the slave frequency. The experimental data was smoothed and normalized and compared to the numerical evaluation of the Fokker-Planck equation (dotted) using the same detuning and locking bandwidth as measured experimentally. Theoretically, as the magnitude of the frequency detuning is increased the overshoot is reduced. This was also observed experimentally.

3) *Effect of frequency detuning on the mean frequency transient:* A typical experimental output is shown in Fig. 15 for a frequency detuning of 250 MHz and a locking bandwidth of 500 MHz. The numerical simulations with the same parameters shows that there should be frequency overshoot for these parameters. However, we did not average on the oscilloscope long enough to see the over-

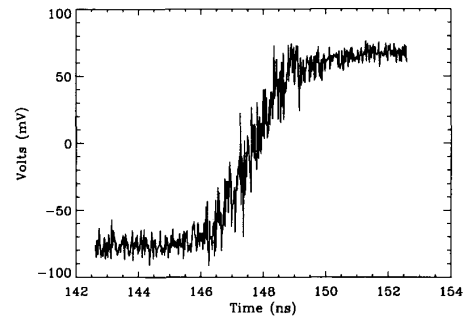


Fig. 15. Typical raw data for detuning effect measurement. $\Delta f_L = 500$ MHz, $\Delta f = 250$ MHz.

shoot. To obtain the experimental results presented earlier which showed the overshoot, we averaged for a few minutes. In this present experiment, we averaged only on the order of 10 to 15 s since averaging for shorter times reduces the effect of the frequency drift on the measurement.

Using a least square method, the raw data shown in Fig. 15 were fitted to a function of the form

$$y = x_1 + x_2 \tanh [x_3 (t + x_4)]. \quad (63)$$

After the function was fitted, it was normalized such that at $t = -\infty$ the function had a value of one, and at $t = \infty$ it had a value of zero. We then recorded the time which corresponded to an output value of 0.5 along with the slope of the function at this point. Then the experiment was repeated until we had collected five data points for the first frequency detuning. At this point, we increased the frequency detuning by 100 MHz and repeated the experiment. The results are shown in Table II. The frequency detuning is shown in the first column of the table. In the second column, the time t_m which corresponds to the output value of 0.5 is listed. The standard deviation of t_m is listed in column three. The last two columns list the slope and standard deviation of the slope evaluated at $t = t_m$. In Fig. 16 we compare the numerical results (dotted) with the time shifted fitted functions (solid). The numerical (dotted) plot closest to the Δf axis is the results obtained using 250 MHz detuning, and the furthest from the axis was obtained with a detuning of 450 MHz. The fitted functions were all time shifted by the same amount.

There are some important points about this comparison which should be discussed. First, the choice of the tanh function as the fitting function is obviously not the best. This functional choice will limit how well the fit to the numerical results will be. Second, the values of the frequency detuning and the locking bandwidth have some uncertainty. This also will affect the fit. We determined that the uncertainty in the locking bandwidth was negligible throughout the experiment and that the frequency difference between successive detunings was 100 ± 20 MHz. Considering the limitations of the fitting functions and the uncertainties in the experimental parameters, the agreement between the model and the experiment is very good.

TABLE II
EFFECT OF FREQUENCY DETUNING ON LOCKING TRANSIENT FOR A LOCKING BANDWIDTH OF 500 MHz.

Δf (MHz)	t_m (ns)	σ_t (ns)	slope at t_m	σ_s
250	147.53	0.09	0.430	0.016
350	148.21	0.11	0.317	0.013
450	148.96	0.16	0.265	0.013

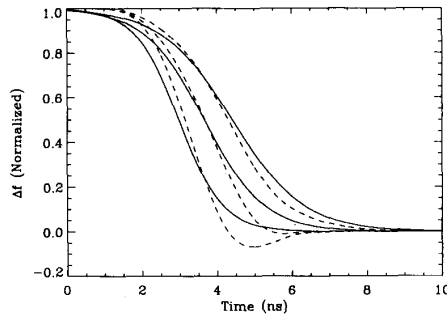


Fig. 16. Comparison of experiment and numerical results of the effect of frequency detuning on the mean frequency transient. The solid line is a tanh fit to the experimental data and the dotted line is a numerical evaluation of the Fokker-Planck equation. $\Delta f_L = 500$ MHz and $\Delta f = 250, 350, 450$ MHz.

4) *Effect of locking bandwidth on the mean frequency transient:* The final experimental result we will present shows the dependence of the mean locking transient on the locking bandwidth. Basically, we are repeating the last experiment, but instead of varying the detuning we varied the locking bandwidth by changing the injection level. This experiment is slightly more difficult because each time the injection level is changed, the pulling effect of the master carrier frequency is also changed. We attempted to measure the pulling due to the carrier for each injection level and compensate the frequency detuning in such a way to always have a detuning of 200 MHz.

The values used in the model for the locking bandwidth were checked by measuring the locking bandwidth at one injection level and assuming it increases as the square root of the injected power. This theoretical result was compared to the measure values of the locking bandwidth and matched well.

The same tanh functional form was used to fit the data and the results are shown in Table III. In Fig. 17 we show the comparison between the numerical evaluation of Fokker-Planck (dotted) with the fitted functions. The numerical (dotted) plot closest to the Δf axis corresponds to a locking bandwidth of 350 MHz, whereas the one furthest from the axis is for a locking bandwidth of 550 MHz.

Again, we stress that the trends predicted by the numerical simulations of the Fokker-Planck equation are what we observed experimentally. That is, as the locking bandwidth was increased, the value of t_m decreased and the slope increased.

TABLE III
EFFECT OF LOCKING BANDWIDTH ON LOCKING TRANSIENT FOR A DETUNING OF 200 MHz.

Δf_L (MHz)	t_m (ns)	σ_t (ns)	slope at t_m	σ_s
350	147.46	0.17	0.310	0.017
440	147.10	0.05	0.436	0.016
550	146.83	0.06	0.506	0.050

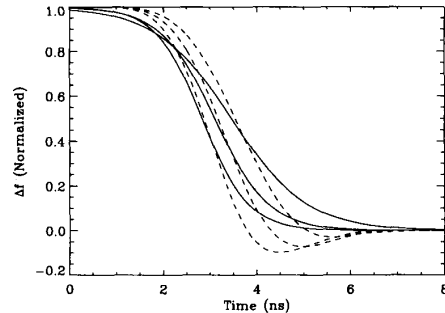


Fig. 17. Comparison of experiment and numerical results of the effect of locking bandwidth on the mean frequency transient. The solid line is a tanh fit to the experimental data and the dotted line is a plot of the numerical evaluation of the Fokker-Planck equation. $\Delta f = 200$ MHz and $\Delta f_L = 350, 440, \text{ and } 550$ MHz.

VI. CONCLUSION

In summary we have presented a detailed theoretical and experimental study of transients of injection locked semiconductor lasers. Particular attention was focused on the effect of noise on the phase transients.

The theoretical model is based on the rate equations including spontaneous emission noise sources. Gain saturation leads to a small correction to the standard steady-state solutions. By adiabatically eliminating the carrier and intensity dynamics, we derived a Langevin equation for the relative phase between the master and slave lasers. This equation is identical to Adler's equation with the addition of a noise term.

The range of validity of the adiabatic elimination was determined by comparing numerical integration of the full rate equations to the analytical solution of Adler's equation. Also, the effect of nonzero injection signal rise time and fall time is important when discussing phase transients. For injection signal rise times significantly longer than the relaxation oscillation period, we found the adiabatic elimination yields accurate results for the phase transients. Setting the rise times to zero will result in exciting relaxation oscillations which can reduce the bandwidth of application utilizing injection locked lasers. However, with nonzero rise and fall times there is much less excitation of relaxation oscillations since the spectrum of a smooth rise (fall) drops off much more quickly than the spectrum of a discontinuity. Therefore, we con-

cluded that nonzero rise and fall times must be considered when investigating limitations on bandwidth of applications utilizing injection locking. In the weak injection limit, Adler's solution was found to be sufficiently accurate even for zero rise times due to the very low excitation of the relaxation oscillations.

The effect of noise on the phase transients was studied using both the stochastic Adler equation and the corresponding Fokker-Planck equation. We numerically solved the Fokker-Planck equation starting from a uniform relative phase distribution and plotted the time evolution of both the probability density function and the relative phase variance. In steady state, the distribution function could be adequately approximated by a Gaussian with a variance given by the laser linewidths, locking bandwidth, and frequency detuning. A power spectral density analysis of the relative phase showed how the observed phase uncertainty could be reduced using a limited bandwidth phase detector.

The analysis showed that the noise plays a major role in two instances. First, we showed that the noise could drastically shorten the transit time for phase transients with initial conditions at or close to the unstable equilibrium points. Second, it was found that even in steady state, the noise could cause the relative phase to jump by 2π . We numerically calculated this mean escape time from the Fokker-Planck equation. Except for detuning very close to the locking bandwidth we found that the escape time could accurately be approximated with the classical Arrhenius formula (or Kramer's escape time) inside the locking bandwidth and with Adler's frequency pulling formula outside the locking bandwidth. This escape time puts a limit on the useful detuning range. For example, with a detuning of 80% of the locking bandwidth the escape time was found to be less than one microsecond.

Throughout this paper we made repeated use of the locking potential. We gained much intuition about phase transients, steady-state distributions, and escape times by considering the relative phase in the locking potential. Adler described a mechanical system which was analogous to injection locking, however, it is difficult to determine the effects of noise from his model. Using the potential described in this paper the effects of noise can be easily determined.

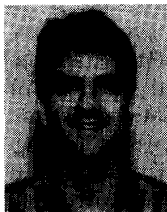
The experimental results confirmed the validity of the theory. We found good agreement between the solutions of the Fokker-Planck equation and the measured average phase transients for a wide range of locking bandwidths and frequency detunings. Even for detailed features such as a frequency overshoot due to the nonzero rise time of the injected signal we found good agreement.

In conclusion, we have determined that the effects of noise on transients in injection locked semiconductor lasers are significant. One must be very aware of the limitations due to noise when considering applications utilizing injection locked semiconductor lasers.

REFERENCES

- [1] B. Van der Pol, "Forced oscillations in a circuit with non-linear resistance," *Phil. Mag.*, vol. 3, pp. 65-80, June 1927.
- [2] R. Adler, "A study of locking phenomena in oscillators," *Proc. IRE*, vol. 34, pp. 351-357, 1946.
- [3] T. White and W. B. Jones, "Frequency transients in synchronized oscillators," *IEEE Trans. Circuit Theory*, vol. 11, pp. 279-281, June 1964.
- [4] R. Lisitsian, "Oscillator locking to the frequency of an external excitation," *Radio Eng. Electron.*, vol. 2, pp. 68-88, Apr. 1957.
- [5] Y. Takayama, "Dynamic behavior of nonlinear power amplifiers in stable and injection-locked modes," *IEEE Trans. Microwave Theory Tech.*, vol. 20, pp. 591-595, Sept. 1972.
- [6] R. Mackey, "Injection locking of klystron oscillators," *IRE Trans. Microwave Theory Tech.*, vol. 10, pp. 228-235, July 1962.
- [7] L. Paciorek, "Injection locking of oscillators," *Proc. IEEE*, vol. 53, pp. 1723-1728, Nov. 1965.
- [8] K. Kurokawa, "Injection locking of microwave solid-state oscillators," *Proc. IEEE*, vol. 61, pp. 1386-1410, Oct. 1973.
- [9] F. Gardner, *Phase-lock Techniques*. 2nd ed. New York: Wiley-Intersci., 1979.
- [10] W. Lindsey, *Synchronization Systems in Communication and Control*. Englewood Cliffs, NJ: Prentice-Hall, 1973.
- [11] H. Stover and W. Steiner, "Locking of laser oscillators by light injection," *Appl. Phys. Lett.*, vol. 8, pp. 91-93, Feb. 1966.
- [12] C. Buczek, R. Freiberg, and M. Skolnick, "Laser injection locking," *Proc. IEEE*, vol. 61, pp. 1411-1431, Oct. 1973.
- [13] S. Kobayashi and T. Kimura, "Coherence of injection-locked AlGaAs semiconductor laser," *Electron. Lett.*, vol. 16, pp. 668-670, Aug. 1980.
- [14] S. Kobayashi, J. Yamada, S. Machida, and T. Kimura, "Single-mode operation of 500 Mbits/s modulated AlGaAs semiconductor laser by injection locking," *Electron. Lett.*, vol. 16, pp. 746-748, Sept. 1980.
- [15] D. Malyn and A. McDonna, "102 km unrepeatereed monomode fibre system experiment at 140 Mbit/s with an injection locked 1.52 μm laser transmitter," *Electron. Lett.*, vol. 18, pp. 445-447, May 1982.
- [16] H. Nishimoto, H. Kuwahara, and M. Motegi, "Injection-locked 1.5 μm InGaAsP/InP lasers capable of 450 Mbit/s transmission over 106 km," *Electron. Lett.*, vol. 19, pp. 509-510, July 1983.
- [17] H. Toba, Y. Kobayashi, K. Yanagimoto, H. Nagai, and M. Nakahara, "Injection-locking technique applied to a 170 km transmission experiment at 445.8 Mbit/s," *Electron. Lett.*, vol. 20, pp. 370-371, Apr. 1984.
- [18] Y. Yamamoto and T. Kimura, "Coherent optical fiber transmission systems," *IEEE J. Quantum Electron.*, vol. QE-17, pp. 919-935, June 1981.
- [19] S. Kobayashi and T. Kimura, "Optical phase modulation in an injection locked AlGaAs semiconductor laser," *IEEE J. Quantum Electron.*, vol. QE-18, pp. 1662-1669, Oct. 1982.
- [20] L. Goldberg, H. Taylor, and J. Weller, "Frequency modulation characteristics of coupled stripe laser diode array," *IEEE J. Quantum Electron.*, vol. 23, pp. 513-526, Apr. 1986.
- [21] L. Goldberg, "Applications of injection-locked narrow stripe and large active area laser diodes," in *Tech. Dig. Ser.*, CLEO 1990.
- [22] G. Elze, G. Grobkopf, L. Kuller, and G. Wenke, "Experiments on modulation properties and optical feedback characteristics of laser diodes stabilized by an external cavity or injection locking," *J. Lightwave Technol.*, vol. LT-2, pp. 1063-1069, Dec. 1984.
- [23] L. Goldberg, "FM sideband injection locking of diode lasers," *Electron. Lett.*, vol. 18, pp. 1019-1020, Nov. 1982.
- [24] —, "Microwave signal generation with injection-locked laser diodes," *Electron. Lett.*, vol. 19, pp. 491-493, June 1983.
- [25] K. Otsuka and S. Tarucha, "Theoretical studies on injection locking and injection-induced modulation of laser diodes," *IEEE J. Quantum Electron.*, vol. QE-17, pp. 1515-1521, Aug. 1981.
- [26] R. Lang, "Injection locking properties of a semiconductor laser," *IEEE J. Quantum Electron.*, vol. 18, pp. 976-983, June 1982.
- [27] F. Mogenssen, H. Olesen, and G. Jacobsen, "Locking conditions and stability properties for a semiconductor laser with external light injections," *IEEE J. Quantum Electron.*, vol. 21, pp. 784-793, July 1985.
- [28] C. Henry, N. Olsson, and N. Dutta, "Locking range and stability of injection locked 1.54 μm InGaAsP semiconductor lasers," *IEEE J. Quantum Electron.*, vol. 21, pp. 1152-1156, Aug. 1985.

- [29] H. Winful and S. Wang, "Stability of phase locking in coupled semiconductor laser arrays," *Appl. Phys. Lett.*, vol. 53, pp. 1894-1896, Nov. 1988.
- [30] J. Tredicce, F. Arecchi, G. Lippi, and G. Puccioni, "Instabilities in lasers with an injected signal," *J. Opt. Soc. Amer. B*, vol. 2, pp. 173-183, Jan. 1985.
- [31] J. Tsacoyeanes, "Phase locking and stability properties for two coupled semiconductor lasers," *J. Appl. Phys.*, vol. 64, pp. 32-36, July 1988.
- [32] L. Goldberg, H. Taylor, and J. Weller, "Locking bandwidth asymmetry in injection-locked GaAlAs lasers," *Electron Lett.*, vol. 18, pp. 986-987, Nov. 1982.
- [33] K. Kobayashi, H. Nishimoto, and R. Lang, "Experimental observation of asymmetric detuning characteristics in semiconductor laser injection locking," *Electron Lett.*, vol. 18, pp. 54-56, Jan. 1982.
- [34] I. Petitbon, P. Gallion, G. Debarge, and C. Chabran, "Locking bandwidth and relaxation oscillations of an injection-locked semiconductor laser," *IEEE J. Quantum Electron.*, vol. 24, pp. 148-154, Feb. 1988.
- [35] M. Lax, "Classical noise IV: Langevin methods," *Rev. Mod. Phys.*, vol. 38, pp. 541-566, July 1966.
- [36] W. Chow, "Theory of line narrowing and frequency selection in an injection locked laser," *IEEE J. Quantum Electron.*, vol. QE-19, pp. 243-249, Feb. 1983.
- [37] F. Mogensen, H. Olesen, and G. Jacobsen, "FM noise suppression and linewidth reduction in an injection-locked semiconductor laser," *Electron Lett.*, vol. 21, pp. 696-697, Aug. 1985.
- [38] K. Kikuchi and C. Zah, "Spectral, phase noise and phase modulation characteristics of AM sideband injection-locked semiconductor lasers," *Electron Lett.*, vol. 23, pp. 437-439, Apr. 1987.
- [39] P. Gallion, H. Nakajima, G. Debarge, and C. Chabran, "Contribution of spontaneous emission to the linewidth of an injection-locked semiconductor laser," *Electron Lett.*, vol. 21, pp. 626-628, July 1985.
- [40] P. Spano, S. Piazzolla, and M. Tamburrini, "Frequency and intensity noise in injection-locked semiconductor lasers: Theory and experiments," *IEEE J. Quantum Electron.*, vol. QE-22, pp. 427-435, Mar. 1986.
- [41] N. Schunk and K. Petermann, "Noise analysis of injection-locked semiconductor injection lasers," *IEEE J. Quantum Electron.*, vol. QE-22, pp. 642-650, May 1986.
- [42] H. A. Haus and Y. Yamamoto, "Quantum noise of an injection-locked laser oscillator," *Phys. Rev. A*, vol. 29, pp. 1261-1274, Mar. 1984.
- [43] B. Tromborg, H. Olesen, X. Pan, and S. Saito, "Transmission line description of optical feedback injection locking for Fabry-Perot and DFB lasers," *IEEE J. Quantum Electron.*, vol. QE-23, pp. 1875-1889, Nov. 1987.
- [44] G. Hadley, "Injection locking of diode lasers," *IEEE J. Quantum Electron.*, vol. QE-22, pp. 419-426, Mar. 1986.
- [45] P. Spano, M. Tamburrini, and S. Piazzola, "Optical FSK modulation using injection locked laser diodes," *J. Lightwave Technol.*, vol. 7, pp. 726-728, Apr. 1989.
- [46] H. Haken, *Light*, vol. 2. Amsterdam: North-Holland Physics, 1985.
- [47] M. Lax, "Fluctuations from the nonequilibrium steady state," *Rev. Mod. Phys.*, vol. 32, pp. 25-64, Jan. 1960.
- [48] C. Henry, "Phase noise in semiconductor lasers," *J. Lightwave Technol.*, vol. LT-4, pp. 298-311, Mar. 1986.
- [49] R. Lang, K. Vahala, and A. Yariv, "The effect of spatially dependent temperature and carrier fluctuations on noise in semiconductor lasers," *IEEE J. Quantum Electron.*, vol. QE-21, pp. 443-451, May 1985.
- [50] C. H. Henry, "Theory of the phase noise and power spectrum of a single mode injection laser," *IEEE J. Quantum Electron.*, vol. QE-19, pp. 1391-1397, Sept. 1983.
- [51] G. Agrawal and N. Dutta, *Long-Wavelength Semiconductor Lasers*. New York: Van Nostrand Reinhold, 1986.
- [52] M. Lax, "Quantum noise VII: The rate equations and amplitude noise in lasers," *IEEE J. Quantum Electron.*, vol. QE-3, pp. 37-46, Feb. 1967.
- [53] G. Arfken, *Mathematical Methods for Physicists*. 3rd ed. New York: Academic, 1985.
- [54] M. Surette, "Noise properties of injection locked semiconductor lasers: Application to optically driven phased array antennas," Ph.D. dissertation, University of Colorado, 1991.
- [55] C. W. Gardiner, *Handbook of Stochastic Methods*. 2nd ed. New York: Springer-Verlag, 1985.
- [56] F. Haake, "Decay of unstable states," *Phys. Rev. Lett.*, vol. 41, pp. 1685-1688, Dec. 1978.
- [57] F. Haake, J. Haus, and R. Glauber, "Passage-time statistics for the decay of unstable equilibrium states," *Phys. Rev. A*, vol. 23, pp. 3255-3271, June 1981.
- [58] F. Arecchi, A. Politi, and L. Ulivi, "Stochastic time approach to the decay of unstable states: failure of the asymptotic approximation," *Phys. Lett.*, vol. 87A, pp. 333-335, Jan. 1982.
- [59] F. Arecchi and A. Politi, "Transient fluctuations in the decay of an unstable state," *Phys. Rev. Lett.*, vol. 45, pp. 1219-1222, Oct. 1980.
- [60] S. Balle, P. Colet, and M. San Miguel, "Statistics for the transient response of single-mode semiconductor laser gain switching," *Phys. Rev. A*, vol. 43, pp. 498-506, Jan. 1991.
- [61] P. Spano, A. D'Ottavi, A. Mecozzi, B. Daino, and S. Piazzolla, "Experimental measurements and theory of first passage time in pulse-modulated semiconductor lasers," *IEEE J. Quantum Electron.*, vol. 25, pp. 1440-1449, June 1989.
- [62] B. Lathi, *Modern Digital and Analog Communication Systems*. New York: Holt, Rinehart and Winston, 1983.
- [63] H. Risken, *The Fokker-Planck Equation*. New York: Springer-Verlag, 1984.
- [64] J. Mork and B. Tromborg, "The mechanism of mode selection for an external cavity laser," *IEEE Photon. Technol. Lett.*, vol. 2, pp. 21-23, Jan. 1990.



Marc R. Surette was born in Brighton, MA, on February 6, 1964. He received the B.S. degree (summa cum laude) in computer systems engineering from the University of Massachusetts, Amherst, in 1986. After a year at IBM Corporation he entered the University of Colorado, Boulder, where he received the M.S. and Ph.D. degrees in electrical engineering in 1989 and 1991, respectively. His doctoral dissertation was on the effects of noise on transients of injection locked semiconductor lasers. He also investigated optically driven phased array antennas and developed numerical models for optical waveguides.

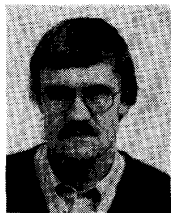
He is currently a post-Doctoral Fellow in the Optical Sciences Division of the Naval Research Laboratory, Washington, DC. His current research interests are in the areas of broad area semiconductor optical amplifiers, semiconductor lasers, and numerical modeling of electrooptical devices.

Dr. Surette is a member of the IEEE Lasers and Electro-Optics Society, the Optical Society of America, Eta Kappa Nu, and Tau Beta Pi.



Dag Roar Hjelme (S'86-M'87) was born in Valldal, Norway, on March 25, 1959. He received the M.S. degree in electrical engineering from the Norwegian Institute of Technology, Trondheim, Norway, in 1982 and the Ph.D. degree in electrical engineering from the University of Colorado, Boulder, in 1988.

From 1983 to 1984, he was with the Norwegian Institute of Technology, Division of Physical Electronics, working on fiber optics and integrated optics. He is currently a post-Doctoral Research Associate with the Department of Electrical and Computer Engineering, University of Colorado. His current research interests include spectral and dynamic properties of semiconductor lasers, ultrafast optics, and electrooptic sampling.



Reinold Ellingsen was born in Soemna, Norway, on April 26, 1951. He received the M.Sc. and Ph.D. degrees, both in electrical engineering, from the Norwegian Institute of Technology (NTH), Trondheim, Norway, in 1977 and 1984, respectively. His dissertation work was on optical and thermal dosimetry during laser induced photochemical and hyperthermal treatment of cancer.

In 1977 he was with the Norwegian Institute of Radiation Hygiene, working on ionizing radiation. From 1978 to 1984 he was with the Institute of Physical Electronics at NTH. Since then he has been with the Electronics Research Laboratory at NTH, working on optical fiber communication, especially on coherent systems. His recent work has focused on laser diode stabilization for reference frequency and optical spectroscopy applications.



Alan Rolf Mickelson (S'72-M'78) was born in Westport, CT, on May 2, 1950. He received the B.S.E.E. degree from the University of Texas, El Paso, in 1973 and the M.S. and Ph.D. degrees from the California Institute of Technology, Pasadena, in 1974 and 1978, respectively.

Following a post-Doctoral period at Caltech in 1980, he joined the Electronics Research Laboratory of the Norwegian Institute of Technology, Trondheim, Norway, at first as an NTN post-Doctoral Fellow, and later as a staff scientist. His research in Norway primarily concerned characterization of optical fibers and fiber compatible components and devices. In 1984 he joined the Department of Electrical and Computer Engineering at the University of Colorado, Boulder, where he became an Associate Professor in 1986. His research presently involves semiconductor laser characterization, integrated optic device fabrication and characterization, and fiber system characterization.